

Parity Violation in Proton-Proton Scattering

A.R. Berdoz^{a,b}, J. Birchall^a, J.D. Bowman^c, J.R. Campbell^a, C.A. Davis^d, A.A. Green^a, P.W. Green^e, A.A. Hamian^a, D.C. Healey^d, R. Helmer^d, S. Kadantsev^f, Y. Kuznetsov^f, R. Laxdal^d, L. Lee^a, C.D.P. Levy^d, R.E. Mischke^c, S.A. Page^a, W.D. Ramsay^a, S.D. Reitzner^a, G. Roy^e, P.W. Schmor^d, A.M. Sekulovich^a, J. Soukup^e, G.M. Stinson^e, T. Stocki^e, V. Sum^a, N.A. Titov^f, W.T.H. van Oers^a, R-J. Woo^a, A.N. Zelenski^f

^aDepartment of Physics, University of Manitoba, Winnipeg MB, Canada R3T 2N2

^bDepartment of Physics, Carnegie Mellon University, Pittsburgh PA, USA 15213

^cLos Alamos National Laboratory, Los Alamos NM, USA 87545

^dTRIUMF, 4004 Wesbrook Mall, Vancouver, B.C., Canada V6T 2A3

^eDepartment of Physics, University of Alberta, Edmonton AB, Canada T5G 2N5

^fInstitute for Nuclear Research, Russian Academy of Sciences, 117312 Moscow, Russia

Presented by Willem T.H. van Oers

Abstract

Measurements of parity-violating longitudinal analyzing powers (normalized asymmetries) in polarized proton-proton scattering provide a unique window on the interplay between the weak and strong interactions between and within hadrons. Several new proton-proton parity violation experiments are presently either being performed or are being prepared for execution in the near future: at TRIUMF at 221 MeV and 450 MeV and at COSY (Kernforschungsanlage Jülich) at 230 MeV and near 1.3 GeV. These experiments are intended to provide stringent constraints on the set of six effective weak meson-nucleon coupling constants, which characterize the weak interaction between hadrons in the energy domain where meson exchange models provide an appropriate description. The 221 MeV is unique in that it selects a single transition amplitude ($^3P_2 - ^1D_2$) and consequently constrains the weak meson-nucleon coupling constant h_p^{pp} . The TRIUMF 221 MeV proton-proton parity violation experiment is described in some detail. A preliminary result for the longitudinal analyzing power is $A_z = (1.1 \pm 0.4 \pm 0.4) \times 10^{-7}$. Further proton-proton parity violation experiments are commented on. The anomaly at 6 GeV/c requires that a new multi-GeV proton-proton parity violation experiment be performed.

One of the more promising ways to study the neutral weak current interaction in hadronic systems is through measurements of parity violation in nucleon-nucleon (N-N)

scattering. In the low-energy region, where meson exchange models provide an adequate description of the strong N-N interaction, an extension can be made to include the weak interaction. Pictorially, the exchanged meson (π , ρ , ω) is emitted at a weak interaction vertex and absorbed at a strong interaction vertex, or vice versa. The weak interaction vertex is calculated from the Weinberg-Salam model with W- and Z-bosons exchanged between intermediate mesons and constituent quarks, treating strong interaction effects in renormalization group theory in the regime of nonperturbative QCD. In a seminal paper following the above approach, restricted to one-boson exchanges, Desplanques, Donoghue and Holstein (DDH) [1] have calculated a set of six weak meson-nucleon coupling constants (a seventh was found to be rather small and is usually neglected). These six weak meson-nucleon coupling constants are denoted: $f_\pi^1, h_\rho^0, h_\rho^1, h_\rho^2, h_\omega^0, h_\omega^1$; where the subscript indicates the exchanged meson and the superscript the isospin change. DDH tabulated “best guess values” and “reasonable ranges”. As shown in Table 1, the “reasonable ranges of values” indicate uncertainties with respect to the “best guess values” of a few hundred percent. Similar calculations have been made by Dubovik and Zenkin (DZ) [2]. Extending the earlier work in the nucleon sector, Feldman, Crawford, Dubach, and Holstein (FCDH) [3] included the weak Δ -nucleon-meson and weak Δ - Δ -meson parity violating vertices for π , ρ , and ω mesons. The latter authors also present both “best guess values” and “reasonable ranges” for the weak meson-nucleon coupling constants. Using the expressions of an earlier paper by Desplanques (D) [4] the latter authors (FCDH) present a third set of weak meson-nucleon coupling constants. It is to be noted that the large ranges of possible theoretical values persist. Taking into account the more recent experiments, Desplanques [5] has argued for a reduced range for the weak meson-nucleon coupling constant f_π^1 . The weak meson-nucleon coupling constants have also been calculated by Kaiser and Meissner (KM) [6] within the framework of a non-linear chiral effective Lagrangian which includes π , ρ , and ω mesons. In this model f_π^1 is considerably smaller than the “best guess value” of DDH or FCDH. Furthermore, a non-zero and non-negligible value for the seventh weak meson-nucleon coupling constant $h_\rho^{\prime 1}$ was found. A complete determination of the six weak meson-nucleon coupling constants requires at least six pieces of independent experimental information. As of to date there do not exist enough experimental constraints of statistical significance to determine the six weak meson-nucleon coupling constants. Consequently, one needs several new precision parity violation measurements.

Impressively precise measurements of the longitudinal analyzing power A_z in p - p scattering have now been made at 13.6 MeV [$A_z = (-0.93 \pm 0.20 \pm 0.05) \times 10^{-7}$] at the University of Bonn [7] and at 45 MeV [$A_z = (-1.57 \pm 0.23) \times 10^{-7}$] at the Paul Scherrer Institute (PSI) [8]. Here A_z is defined as $A_z = (\sigma^+ - \sigma^-)/(\sigma^+ + \sigma^-)$, where σ^+ and σ^- represent the scattering cross section for polarized incident protons of positive and negative helicity, respectively, integrated over a range of angles determined by the acceptance of the particular experimental apparatus. A non-zero value of A_z implies parity violation due to the non-zero pseudo-scalar observable $\vec{\sigma} \cdot \vec{p}$ with $\vec{\sigma}$ the spin and \vec{p} the momentum of the incident proton. From the PSI measurement at 45 MeV and the \sqrt{E} energy dependence of A_z at lower energies, one can extrapolate A_z at 13.6 MeV to be $A_z = (-0.86 \pm 0.13) \times 10^{-7}$. There exists thus excellent agreement between the above two lower energy measurements. Both results allow pinning down a combination of the effective ρ and ω weak meson-nucleon coupling constants h_ρ^{pp} and h_ω^{pp} , with $h_\rho^{pp} = h_\rho^0 + h_\rho^1 + \frac{h_\rho^2}{\sqrt{6}}$ and $h_\omega^{pp} =$

$h_\omega^0 + h_\omega^1$. It should be noted that a measurement of A_z in p - p scattering is sensitive only to the short range part of the parity violating interaction (parity violating π^0 exchange would simultaneously imply CP violation and is therefore suppressed). Following the approach of Adelberger and Haxton [9], one can fit the more significant nuclear parity violation data using theoretical constraints by the two parameters f_π^1 and $(h_\rho^0 + 0.6 \times h_\omega^0)$. This leaves the experimental value of $f_\pi^1 = (0.28_{-0.28}^{+0.89}) \times 10^{-7}$ [10] at the border of the deduced range so determined [11]. See Table 1, last two columns.

A partial wave decomposition allows the various contributions to A_z to be calculated based upon reasonable estimates of the parity violating mixing angles [12]. These mixing angles are directly related to the parity violating transition amplitudes ($^1S_0 - ^3P_0$), ($^3P_2 - ^1D_2$), ($^1D_2 - ^3F_2$), ($^3F_4 - ^1G_4$), etc. The energy dependence of the first two parity violating transition amplitudes contributing to A_z is shown in Fig. 1 [13]. For energies below 100 MeV essentially only the first parity violating transition amplitude ($^1S_0 - ^3P_0$) contributes. One notices the increase in importance of the second parity violating transition amplitude for energies above 100 MeV. There exists a further p - p parity violation measurement at 800 MeV with $A_z = (2.4 \pm 1.1) \times 10^{-7}$ [14]. Interpretation of the latter result in terms of the effective ρ and ω weak meson-nucleon coupling constants is more difficult due to the presence of a large inelasticity (pion production).

As shown in Fig. 1 there is a unique feature at an energy of 230 MeV: the ($^1S_0 - ^3P_0$) transition amplitude contribution integrates to zero. This reflects a change in sign of both the 1S_0 and 3P_0 strong interaction phases near 230 MeV and is completely independent of the weak meson-nucleon coupling constants. The absolute scale and sign of the ordinate are determined by the weak interaction. Neglecting a small contribution ($\sim 5\%$) from the ($^1D_2 - ^3F_2$) transition amplitude, a measurement of A_z at 230 MeV constitutes a measurement of the ($^3P_2 - ^1D_2$) transition amplitude. Simonius [15] has shown that the ($^3P_2 - ^1D_2$) transition amplitude depends only weakly on ω -exchange (to an extent dependent on the choice of the vector meson-nucleon coupling constants of various $N - N$ potential models), whereas ρ -exchange and ω -exchange contribute to the ($^1S_0 - ^3P_0$) transition amplitude with equal weight. Therefore, a measurement of A_z at an energy of 230 MeV constitutes a determination of h_ρ^{pp} .

Various theoretical predictions of the longitudinal analyzing power have been reported; at 230 MeV the values of A_z are $+0.7 \times 10^{-7}$ [16], $+0.6 \times 10^{-7}$ [13], and $+0.4 \times 10^{-7}$ [17]. Extensions to the one-boson exchange model have been made to include 2π and $\pi - \rho$ exchanges via $N-\Delta$ and $\Delta-\Delta$ intermediate states to which the ($^3P_2 - ^1D_2$) transition amplitude is particularly sensitive. For instance, Iqbal and Niskanen [16] find that the Δ isobar contribution at 230 MeV (dependent on f_π^1) may be as large as the single ρ -exchange contribution, enhancing the value of A_z by a factor of two. What is required is a self-consistent theoretical calculation of the longitudinal analyzing power A_z , avoiding possible double counting and taking into account that the value of f_π^1 is constrained by experiment to be rather small. Considering all the above, a measurement of A_z at 230 MeV to an accuracy of $\pm 2 \times 10^{-8}$ would provide a most important determination of parity violation in p - p scattering.

In the current TRIUMF experiment, a 200 nA proton beam with a polarization of 0.80 to 0.82, extracted from the optically pumped polarized ion source (OPPIS), after passing

Table 1.
Weak meson-nucleon couplings constants

Coupling	Theoretical						Experimental		
	range	'best value'	value	range	'best value'	value	value	best fit	range
	(DDH)	(DDH)	(DZ)	(FCDH)	(FCDH)	(D)	(KM)		
f_π^1	0→11.4	4.6	1.1	0→6.5	2.7	2.7	0.19	2.3	0→11
h_ρ^0	-31→11.4	-11.4	-8.4	-31→11	-3.8	-6.1	-1.9	-5.7	-31→11
h_ρ^1	-0.38→0	-0.19	0.38	-1.1→0.4	-0.4	-0.4	-0.02	-0.2	-0.4→0.0
h_ρ^2	-11.0→-7.6	-9.5	-6.8	-9.5→-6.1	-6.8	-6.8	-3.8	-7.6	-11→-7.6
h_ω^0	-10.3→5.7	-1.9	-3.8	-10.6→2.7	-4.9	-6.5	-1.1	-4.9	-10→5.7
h_ω^1	-1.9→-0.8	-1.1	-2.2	-3.8→-1.1	-2.3	-2.3	-1.0	-0.6	-1.9→-0.8

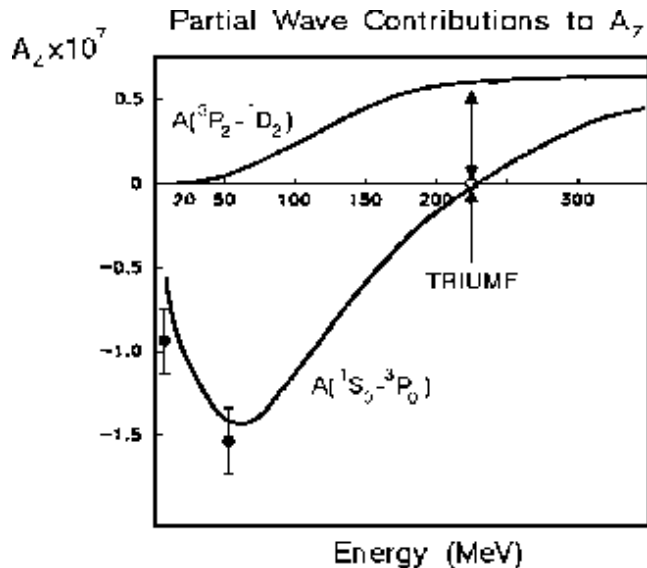


Figure 1. Partial wave decomposition of the p - p parity violating longitudinal analyzing power A_z [Ref.13].

a Wien filter in the injection line is accelerated through the cyclotron to an energy of 221.3 MeV. A combination of solenoid-dipole-solenoid-dipole magnets on the external beam line provides a longitudinally polarized beam with positive or negative helicity. The longitudinal analyzing power A_z follows from the helicity dependence of the p - p total cross section as determined in precise measurements of the normalized transmission asymmetry through a 0.40 m long liquid hydrogen (LH₂) target: $A_z = -(1/P)(T/S)(T^+ - T^-)/(T^+ + T^-)$, where P is the incident beam longitudinal polarization, $T = 1 - S$ is the average transmission through the target, and the + and - signs indicate the helicity state.

There are many other effects that can cause a helicity correlated change in transmission. Very strict constraints are imposed on the incident polarized beam in terms of helicity correlated changes in intensity, in transverse x (horizontal) and y (vertical) beam position and direction, in beam width (given by σ_x and σ_y), and in energy, and further transverse polarizations (given by P_x and P_y), and first moments of transverse polarizations (given by $\langle xP_y \rangle$ and $\langle yP_x \rangle$), together with deviations of the transmission measuring apparatus from cylindrical symmetry. Systematic errors arising from the imperfections of the incident beam and the response of the transmission measuring apparatus are individually not to exceed one tenth of the expected value of A_z (or 6×10^{-9}). Potentially particular troublesome are residual transverse polarizations and their first moments (so called "circulating" polarization profiles), as well as helicity correlated energy changes. Uncorrelated fluctuations contribute to the rms noise in the measurement and increase the total data taking time. In addition to imposing strict constraints on the incident beam and on the measurement apparatus in order to reduce systematic errors, the approach which is being followed is to further measure the sensitivity or response to residual imperfections, to monitor these imperfections during data taking and to make corrections as appropriate.

Helicity changes are implemented through shifts in the linearly polarized laser light

frequency, minimizing helicity correlated changes in the accelerated beam properties. The beam parameters are selected to produce an achromatic waist at the LH₂ target, circular in cross section ($\sigma_x = \sigma_y = 6$ mm). To negate possible helicity correlated changes in the incident beam energy, the currents in the two solenoid magnets as well as the rotation angles around the beam axis of three sets of quadrupole magnets are switched in polarity once every three days. This allows for a linear combination of all four permutations of helicity states from the polarized ion source to the parity violation measurement apparatus in the deduction of A_z . In the cyclotron the spin direction is either parallel or antiparallel to the guide magnetic field. Helicity changes are made in a semi-random eight-state cycle, which is designed to cancel out slow drifts in various beam properties.

Producing a longitudinally polarized beam for the parity violation experiment requires careful tuning of the polarized ion source, of the injection beam line, of the acceleration through the cyclotron, and of the beam transport line to the parity violation measuring apparatus. Many improvements to the operation of the polarized source had to be made to reduce helicity correlated changes in intensity, emittance, polarization, and energy. The Faraday effect provides a means to monitor and control the polarization of the Rubidium vapour (source of the polarized electrons which are exchanged with the passing protons) on line using a probe laser. The polarization direction of the linearly polarized probe laser light is rotated by an angle proportional to the Rubidium vapour polarization. The polarizations of the Rubidium vapour in the two helicity states are maintained to be the same within 0.5% close to 100%. The Faraday rotation measurement also provides confirmation of the helicity state at the polarized ion source.

To aid in tuning, various retractable horizontal and vertical wire chambers were placed along the beam line. Following the second solenoid magnet, where the polarization direction has both a longitudinal and a horizontal sideways component, a four branch polarimeter measures the transverse polarization components, while a beam energy monitor measures the relative energy of the proton beam with a precision of ± 20 keV during a one hour data taking run. The absolute energy has to agree within a few MeV with the energy for which the contribution of the ($^1S_0 - ^3P_0$) transition amplitude integrates to zero, taking into account the finite geometry of the transmission measuring apparatus; but any changes in energy greater than 40 keV will introduce transverse polarization components in excess of 0.001 for the canonical setting of all beam transport magnetic elements. All beam transport elements have their excitations monitored on a continuous basis (superconducting solenoids - currents; dipole magnets using NMR probes; quadrupole magnets using Hall probes).

Figure 2 provides a diagram of the downstream part of the experimental setup. The longitudinally polarized beam, incident from the lower right, passes first a series of diagnostic devices - a set of three beam intensity profile monitors (IPMs), and a pair of transverse polarization profile monitors (PPMs) - before reaching the LH₂ target which is preceded and followed by transverse electric field ionization chambers (TRICs) to measure the beam current.

The IPMs, which are based on secondary electron emission from thin, 3 μm thick nickel foils placed between 8 μm aluminum high voltage foils, measure the beam intensity profile

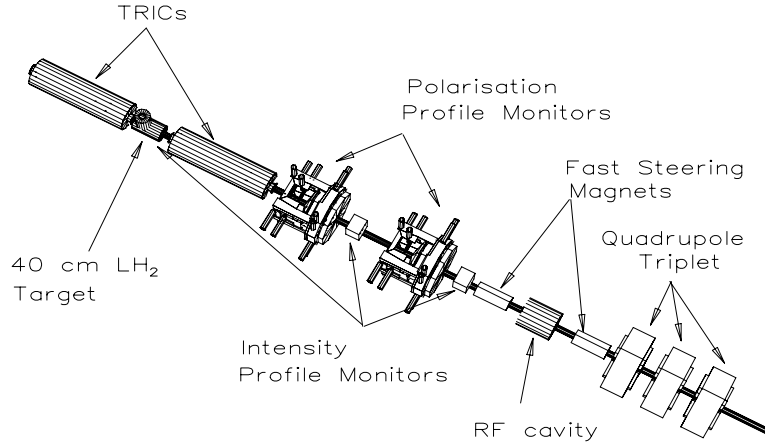


Figure 2. Three dimensional view of the TRIUMF parity violation detection apparatus.

with harps of 31 foil strips (1.5 mm wide, separated 2.0 mm center to center) in both the vertical (x-profile) and horizontal (y-profile) directions. The third IPM placed just in front of the LH₂ target has 10 μm thick nickel strips (2.5 mm wide, separated by 3.0 mm center to center). Beam centroid evaluators determine the beam intensity profile centroids on line at two locations through appropriate integration of the discrete distributions; a corresponding normalized error signal is used to drive feedback loops to x and y, ferrite-cored fast steering magnets. This allows the beam intensity profile centroids to be kept fixed within 1 μm with an offset less than 20 μm from the “neutral axis” in both x and y during a one hour data taking run. Typical beam intensity profile widths are: IPM-1 $\sigma_x = \sigma_y = 5$ mm; IPM-2 : 4 mm; IPM-3 : 6 mm. Sensitivities to helicity correlated position and size modulations are determined with enhanced modulations synchronized to the helicity sequence for the experiment. Position and size modulations are measured during the course of data taking to allow for offline corrections. Typical values of these modulations in a one hour data taking run are $\Delta x, \Delta y < (0.5 \pm 0.3) \mu\text{m}$ and $\Delta\sigma_x, \Delta\sigma_y < (1.0 \pm 0.6) \mu\text{m}$.

The PPMs are based on p - p scattering using CH₂ targets. Scattered protons are detected in a forward arm at 17.5° with respect to the incident beam direction with a pair of scintillation counters. The solid angle defining scintillator is rotated around an axis perpendicular to the scattering plane to compensate for changes in solid angle and differential cross section when the CH₂ target blade moves through the beam (see Fig. 3). Coincident recoil protons are detected in a backward arm at 70.6° with respect to the incident beam direction with a recoil scintillation counter; a second scintillation counter acts as a veto for higher energy protons from $^{12}\text{C}(p,p)X$. Each PPM contains detector assemblies for “left” scattered protons, “right” scattered protons; “down” scattered protons, and “up” scattered protons. The targets consist of CH₂ blades, 1.6 mm wide and 5.0 mm deep along the incident beam direction. The blades move through the beam on a circle of 0.215 m at a frequency of 5 Hz. Each PPM has four blades: two which scan the polarization profile in the horizontal direction and allow for determining the quantity $(L - R)/(L + R)$ and therefore P_y as function of x for each of the two helicity states, and two which scan the polarization profile in the vertical direction and allow for determining the quantity $(D - U)/(D + U)$ and therefore P_x as function of y for each of the two helicity states. Residual

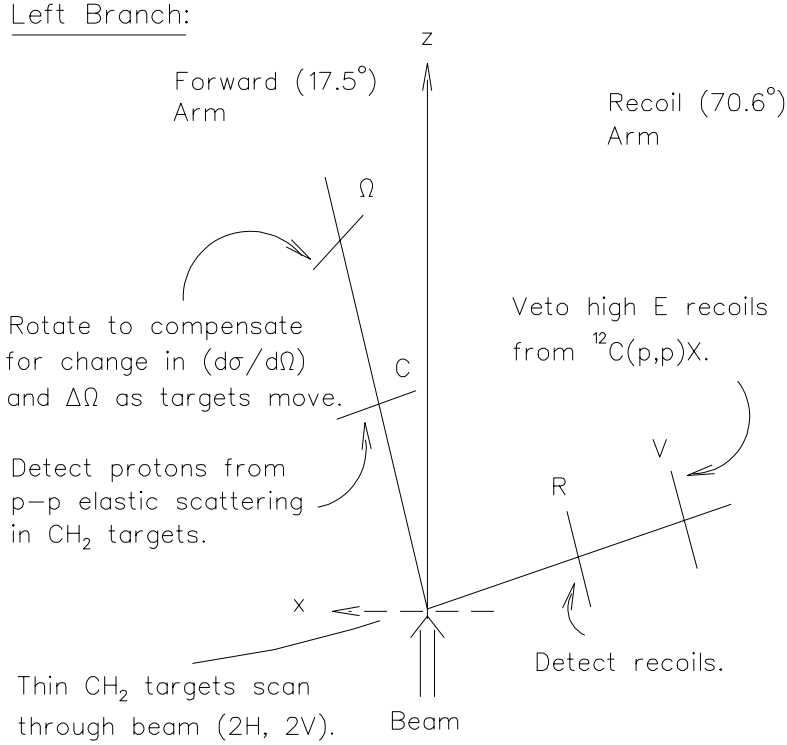


Figure 3. Schematic representation of one of the four detector assemblies of each PPM.

transverse polarizations (which change sign with helicity reversals) can cause a false A_z via the parity allowed transverse analyzing power which produces asymmetric scattering in the LH_2 target. The sensitivities to residual transverse polarizations are dependent on the incident beam position and on the geometry of the parity violation detection apparatus. Both the sensitivities and the “neutral axis” are determined by introducing enhanced transverse polarizations P_x and P_y . The first moments of the transverse polarizations, $\langle xP_y \rangle$ and $\langle yP_x \rangle$, can arise from an inhomogeneous polarization distribution of the cyclotron beam at the stripper foil location and spin precession in the magnetic field gradients at the entrance and exit of solenoids, dipole magnets, and quadrupole magnets. The first moments of the transverse polarizations are $\leq (20 \pm 5) \mu\text{m}$ as measured in a one hour data taking run. The first moments scale with beam size and are minimal at a waist of the incident proton beam. Consequently, the beam transport parameters were chosen so as to have a waist of the incident proton beam at the LH_2 target.

With two PPMs each with four blades, the spin flip or helicity change becomes 40 Hz, i.e., in one cycle all eight blades of the two synchronized PPMs (four blades of PPM-1 and then four blades of PPM-2) will have passed once through the beam. The master clock for sequencing the whole experiment, including helicity changes, is derived from the PPM shaft encoders. In order to suppress the effects of uncorrelated fluctuations in the beam properties up to second order, a cycle consists of the following sequence of helicities: $+ - - + - + + -$, lasting 200 ms. Eight cycles are repeated, with the first helicity chosen so as to form an eight by eight symmetric matrix of helicity states (designated a super-cycle). After four such super-cycles, the pumping laser light is blocked by a shutter during one super-cycle for control measurements. In every other super-cycle of the latter, the sensitivity to helicity correlated changes in the incident beam intensity is

measured using a fourth laser which through photodetachment removes up to 0.2% of the H^- ion beam in the injection line with the 40 Hz frequency. Helicity correlated changes in the incident beam intensity cause a false parity violation signal due to nonlinearities of the TRICs and the associated electronics. Precision analog subtraction of the two TRIC currents minimizes the sensitivity of A_z to $\Delta I/I$. Careful tuning of OPPIS gives values of $\Delta I/I = (2 \pm 1) \times 10^{-5}$ typically in a one hour data taking run. Coherent intensity modulations of up to 0.2% allow for tuning of the analog subtractor for minimum sensitivity at 200 nA and for determining the sensitivity for offline correction of the data. Of each helicity state of 25 ms duration a little more than 1 ms is reserved for the polarization to stabilize following a helicity change, the next 6.4 ms is reserved for the measurement of the transverse polarization (one of the CH_2 blades whisking through the beam), and the following 1/60 sec is used for the actual parity violation measurement (determining the helicity dependent transmission). A small phase slip is introduced so that the master clock and the line frequency are again precisely in phase after 20 minutes.

The LH_2 target has a flask of 0.10 m diameter and a length of 0.40 m. Special precautions have been taken to make the end windows of the target flask perfectly flat and parallel. Maximum heat load of the target is 25 W with operation at 5 W. By circulating the liquid hydrogen rapidly, density gradients are minimized. The target flask is movable remotely within ± 5 mm in two orthogonal directions at both ends to position it on the “neutral axis”. The total scattering probability at 221.3 MeV by the 0.40 m long LH_2 target is close to 4%. The target flask length is limited by multiple Coulomb scattering considerations; the various entrance and exit windows (and all energy degrading foils in the beam) are kept to the minimally allowable thickness.

The main detectors are two transverse electric field ionization chambers, producing current signals due to direct ionization of the ultra-high purity hydrogen gas by the beam. Field shaping electrodes plus guard rings ensure a 0.15 m wide, by 0.15 m high, by 0.60 m long sense region between the parallel electrodes (negatively charged cathode and signal plate), with the field lines all parallel and perpendicular to the electrodes. The TRICs have been designed for operation at -35 kV at one atmosphere; in practise they are operated at a pressure of 150 torr and a high voltage of -8 kV. The entrance and exit windows are located at approximately 0.9 m from the center of the TRICs to range out spallation products from proton interactions with the stainless steel windows. The design of the TRICs incorporated considerations of noise due to δ -ray production and due to recombination.

The proton beam energy in the downstream TRIC is on average 27 MeV lower than in the upstream TRIC due to energy loss in the LH_2 target. Helicity correlated energy modulations will cause a false A_z due to the energy dependence of the energy loss in the hydrogen gas of the TRICs. The sensitivity to coherent energy modulations was determined using a RF accelerating cavity placed upstream of IPM-1 in the beam line. The RF cavity could produce coherent energy modulations up to 1000 eV in the 221.3 MeV proton beam. The measured sensitivity of $(2.9 \pm 0.3) \times 10^{-8} \text{ eV}^{-1}$ agrees very well with the prediction obtained in Monte Carlo simulations of the experiment of $2.8 \times 10^{-8} \text{ eV}^{-1}$ and places a very stringent constraint on the maximally allowable helicity correlated energy modulation of the incident proton beam. Since such an energy modulation cannot be measured directly during parity violation data taking, the false A_z needs to be removed

through an appropriate linear combination of the data taken with all possible helicity combinations and spin precessions. Helicity correlated energy modulations can originate in OPPIS and during acceleration in the cyclotron. Amplification of the former during acceleration in the cyclotron is reduced significantly using a position feedback system in the injection beam line. The naturally occurring coherent energy modulation in OPPIS is measured regularly and is typically less than 20 meV.

The achieved quality of the polarized proton beam at the parity violation data taking apparatus and the performance of the latter will allow for a statistical precision in A_z of $\pm 2 \times 10^{-8}$ in about 300 hours. One fifth of the required data was acquired during four weeks in February-March 1997. A preliminary result for the longitudinal analyzing power at 221.3 MeV is $A_z = (1.07 \pm 0.41 \pm 0.37) \times 10^{-7}$, where the first error is statistical and the second error represents the systematic uncertainty. The result is shown together with the theoretical prediction of Driscoll and Miller [17] in Fig. 4. Even though the theoretical prediction overestimates the size of A_z at the lower energies, it shows the expected energy behavior. Data taking for the 221.3 MeV experiment will continue during several scheduled running periods.

A further p - p parity violation experiment is being prepared at TRIUMF at an energy of 450 MeV [18]. This measurement can be made with minimal changes to the apparatus used in the present TRIUMF p - p parity violation experiment. It is intended to arrive at the same overall uncertainty of $\pm 2 \times 10^{-8}$. The combination of measurements at 221 MeV and 450 MeV would give an independent determination of the weak meson-nucleon coupling constants h_ρ^{pp} and h_ω^{pp} . Measurements of A_z in p - p scattering are also planned at COSY of the Kernforschungsanlage Jülich near 230 MeV and with an extension to 1.3 GeV [19]. The choice of the latter energy (or better a higher energy) is in part motivated by the earlier 5.13 GeV measurement of the longitudinal analyzing power A_z (on a water target) at the ZGS of Argonne National Laboratory, which resulted in $A_z = (26.5 \pm 6.0 \pm 3.6) \times 10^{-7}$ [20]. The result is an order of magnitude larger than what is expected using conventional scaling arguments. It must be remarked that various reevaluations of the experiment have not discovered any flaw, in the way the experiment was conducted, that could have led to such a false large A_z . It has also been pointed out that when Glauber shadowing is taken into account, the fundamental p - p parity violating A_z increases by as much as 40% [21]. Figure 5 shows the energy dependence of A_z ; note the logarithmic scale used for the abscissa. The theoretical prediction for the higher energies [23] was normalized to the 5.13 GeV datum. This calculation is based on a di-quark model introducing a parity violating component of the nucleon wave function. Goldman and Preston find an important role for diagrams in which the weak interaction between the members of a vector di-quark in the polarized proton is accompanied by the strong interaction between that di-quark and a quark of the other proton. The theoretical prediction agrees with the 800 MeV experimental datum and is characterized by a steep increase with increasing energy. It predicts a value for A_z at 20 GeV of the order 10^{-5} . Note that a 200 GeV experiment has placed an upper limit (95% C.L.) on the p - p longitudinal analyzing power A_z of 5.7×10^{-5} [24]. The theoretical interpretation of the unexpectedly large result at 5.13 GeV has created a great deal of controversy [25]. Clearly, the 5.13 GeV result presents a great challenge both in obtaining experimental confirmation through a new

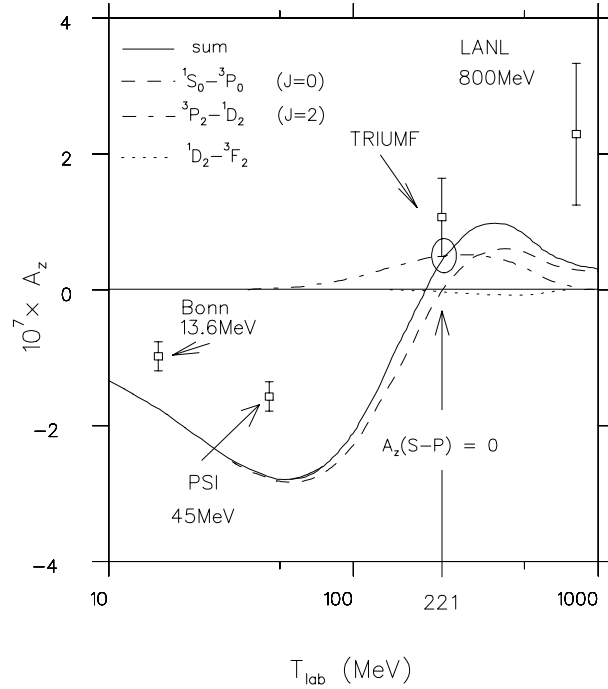


Figure 4. Partial wave decomposition giving the first three contributions to A_z as given by Driscoll and Miller [Ref.17] compared to the experimental data. Note the zero-crossing of the ($^1S_0 - ^3P_0$) transition amplitude contribution.

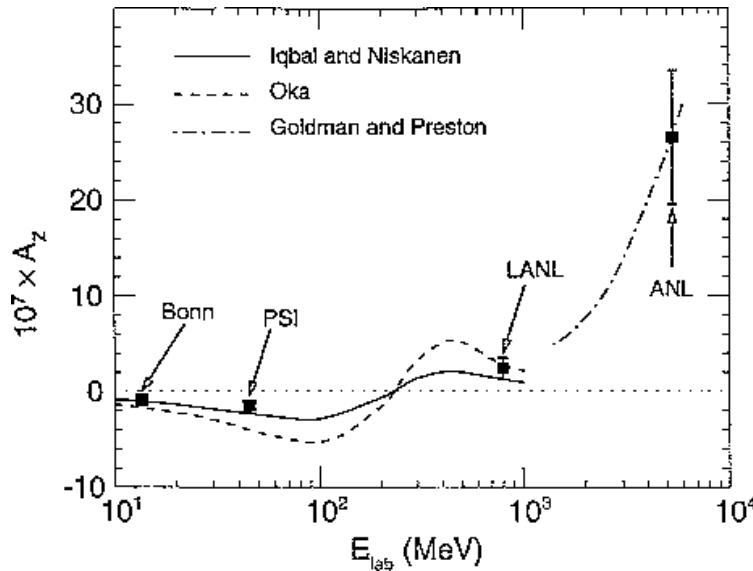


Figure 5. Energy dependence of the p - p parity violating longitudinal analyzing power A_z . The solid and dashed curves represent theoretical models [Ref. 16 and 22] based on weak meson exchange; the dot-dashed curve is described in the text.

measurement at 5 GeV and in obtaining a self-consistent theoretical explanation. If confirmed experimentally, there is a need for a further experiment at an energy of tens of GeV either in a fixed target arrangement or in a storage ring environment.

REFERENCES

- [*] Work supported in part by the Natural Sciences and Engineering Research Council of Canada
1. B. Desplanques, J.F. Donoghue, and B.R. Holstein, *Ann. Phys. (N.Y.)* 124, 449 (1980).
 2. V.M. Dubovik and S.V. Zenkin, *Ann. Phys. (N.Y.)* 172, 100 (1986).
 3. G.B. Feldman, *et al.*, *Phys. Rev. C* 43, 449 (1980).
 4. B. Desplanques, *Nucl. Phys. A* 335, 147 (1980).
 5. B. Desplanques, in *Proceedings of the International Workshop on Parity Violation and Time Reversal Invariance*, ed. N. Auerbach and J.D. Bowman (World Scientific, Singapore, 1996), p. 98
 6. N. Kaiser and U.G. Meissner, *Nucl. Phys. A* 499, 699 (1989); *A* 510, 759 (1990).
 7. P.D. Eversheim, *et al.*, *Phys. Lett. B* 256, 11 (1991); P.D. Eversheim, private communication (1994).
 8. S. Kistryn, *et al.*, *Phys. Rev. Lett.* 58, 1616 (1987).
 9. E.G. Adelberger and W.C. Haxton, *Ann. Rev. Nucl. Part. Sci.* 35, 501 (1985).
 10. W. Haeberli and B.R. Holstein, in *Symmetries and Fundamental Interactions in Nuclei*, ed. W.C. Haxton and E.M. Henley (World Scientific, Singapore, 1995), p. 17.
 11. H.C. Evans, *et al.*, *Phys. Rev. Lett.* 55, 791 (1985); S.A. Page, *et al.*, *Phys. Rev. C* 35, 1119 (1987); M. Bini, *et al.*, *Phys. Rev. Lett.* 55, 795 (1985); *Phys. Rev. C* 38, 1195 (1988).
 12. J. Birchall, G. Roy, and W.T.H. van Oers, *Phys. Rev. D* 37, 1769 (1988).
 13. M. Simonius, in *Proceedings of the Symposium/Workshop on Spin and Symmetries*, ed. W.D. Ramsay and W.T.H. van Oers, *Can. J. Phys.* 66, 245 (1988); F. Nessi-Tedaldi and M. Simonius, *Phys. Lett. B* 215, 159 (1988).
 14. V. Yuan, *et al.*, *Phys. Rev. Lett.* 57, 1680 (1986).
 15. M. Simonius, in *Interaction Studies in Nuclei*, ed. H. Jochim and B. Ziegler (North Holland, Amsterdam, 1975), pp. 3; in *High Energy Physics with Polarized Beams and Targets*, ed. C. Joseph and J. Soffer (Birkhauser Verlag, Basel, 1981), p. 355.
 16. M.J. Iqbal and J. Niskanen, *Phys. Rev. C* 42, 1872 (1990); private communication (1994).
 17. D.E. Driscoll and G.A. Miller, *Phys. Rev. C* 39, 1951 (1989).
 18. TRIUMF Proposal E761, J. Birchall, S.A. Page, and W.T.H. van Oers, *cospokespersons*.
 19. P.D. Eversheim, *et al.* in *High Energy Spin Physics*, ed. K-H. Althoff and W. Meyer (Springer Verlag, Berlin, 1991), p. 573.
 20. N. Lockyer, *et al.*, *Phys. Rev. D* 30, 860 (1984).
 21. L.L. Frankfurt and M.I. Strikman, *Phys. Lett.* 107B, 99 (1981).
 22. T. Oka, *Prog. Theor. Phys.* 66, 977 (1981).
 23. T. Goldman and D. Preston, *Phys. Lett. B* 168, 415 (1986).
 24. D.P. Grosnick, *et al.*, *Phys. Rev. D* 55, 1159 (1997).
 25. M. Simonius and L. Unger, *Phys. Lett. B* 198, 547 (1987); T. Goldman, in *Future Directions in Particle and Nuclear Physics at Multi-GeV Hadron Facilities*, ed. D.F. Geesaman (Brookhaven National Laboratory Report BNL-52389, 1993), p. 140; M. Simonius, *ibid.*, p. 147.